JOURNAL OF MATERIALS SCIENCE 31 (1996) 413–422

Fracture strength and toughness of some phenolic concretes

A. A. SHARIATMADARI, T. V. PARRY*, G. M. PARTON
School of Engineering, University Science Laboratories, South Road, Durham, DH1 3LE, UK

The strength and toughness of a range of phenolic resin based concretes have been evaluated as a function of matrix resin type, content and catalyst ratios. Two resin systems were examined using resin: filler ratios of 4:1, 5:1, 6:1, 7:1 and 8:1 by weight. Catalyst ratios were varied between 4 and 10% by weight of total resin. Through grading mixes were designed using four single sized silica sands of nominal particle sizes 2.4 and 1.2 mm and also 600 and 300 μm in combination with a microfiller with a maximum particle size of 150 μm. Gap gradings were also produced using two of the sand components (1.2 mm and 300 μm) and the microfiller. Microfillers employed included silica flour, china clay and spheriglass 5000. Strength ranged from 4.7 to 7.9 MPa measured in axial tension and 21.3 to 31.4 MPa measured in flexure using four point bending. Fracture toughness, evaluated as the critical strain energy release rate, G_{Ic}, was determined using precracked double torsion specimens. Typical values ranged from 0.13 to 0.22 kJm^{-2}.

1. Introduction

The need for improved strength, toughness, ductility and durability of conventional cement based concretes has, in some circumstances, led to the use of a range of siliceous materials in combination with a polymeric matrix [1–9]. Improved systems have been developed to compete with conventional cement based concrete, which can also exhibit better cost–property ratios [10]. Polymer concrete systems are, however, relatively new to the construction industry, although they differ only from traditional structural concrete by use of a polymer as the cementing or impregnating agent and can be cast into moulds in much the same way [10].

The range of suitable polymers available provides versatility in that a wide variety of fillers may be incorporated into the matrix to adjust its properties. If a polymeric resin is used instead of cement paste to make a precast structural element, it could be potentially lighter in weight, easier to handle and install and also give other characteristics not normally found in cementitious materials. As a result of increasing interest and growing use of polymer concrete, a wide range of applications has been or is now being commercialized generally throughout the world. The resulting products can be both tough and durable.

A major drawback with the use of polymers in many areas is their behaviour in the presence of a fire. Although "fire retarding" resins can be used in critical applications, polymer concretes must generally be considered to be combustible. Considerable quantities of dense and frequently toxic fumes are emitted while burning and their use must therefore be restricted to situations where this disadvantage is not critical. For this reason, much attention has been given to phenolic resin based concrete. It is derived from continuously available raw materials and has been shown to possess equivalent mechanical properties and superior fire and chemical resistance to all other types of resin concrete developed to date [11–13]. Generally, phenolic resin based products are extremely difficult to ignite and do not readily support combustion. When burning, there is very low smoke evolution combined with the minimal emission of toxic fumes. They are high temperature performance materials, have good resistance to corrosion and microbiological attack, do not absorb water and have high resistance to attack by a range of common chemicals.

This paper describes some important mechanical properties achieved for a range of formulations, highlighting the factors which influence optimum strength, as measured by flexural and tensile tests. Fracture toughness, evaluated as the critical strain energy release rate, G_{Ic}, has also been assessed by linear elastic fracture mechanics methods using the double torsion test geometry. This method has been successfully used to determine G_{Ic} for a variety of brittle materials in monolithic and joint form, for which the machining of more complex test geometries would be extremely difficult [14, 15].

2. Experimental procedure

2.1. Mix preparation

All specimens described in this paper were cast from carefully calculated and measured quantities of phenolic resin and granular fillers. The resins employed

* *Present address*: Dr J. H. Burgoyne & Partners, Consulting Scientists and Engineers, Burgoyne House, Chantry Drive, Ilkley, West Yorkshire, LS29 9H0 UK.

0022–2461

were either BP Chemicals' J50/010L (resin A) with proprietary acid catalyst Phencat 15 and/or Forduth Chemicals' IR1271 (resin B) and proprietary acid catalyst CS30.

The granular fillers comprised of a coarse filler, invariably silica sands, and a fine filler referred to as a microfiller, such as silica flour, and were both chosen to be compatible with the particular phenolic resin. The proportionate weight of the sands and microfiller for each formulation was designed to achieve a target grading of either "through" grading or a "gap" grading [16]. The particle fractions present were designed to produce a mix of greatest density which required the minimum amount of resin. To achieve a "through" grading, the mix was designed by combining four "single size" silica sand components with nominal particle sizes of 2.4 and 1.2 mm and also 600 and 300 μm and a microfiller with maximum particle size of 150 μm (Table I). "Gap" grading was obtained by combining two sand components (1.2 mm and 300 μm) and a microfiller (See Table I). A computer program based on a "least squares" method was adopted to calculate the optimum combinations during the design stage of the mix preparation [17]. Good quality silica sands were selected thus enabling easy mixing and handling. The particular sizes were selected for two reasons. First, the production of microproducts requires a microresin concrete and, second, silica sands in the range used contained least impurities with minimum silica (SiO_2) content of 97%.

To study the influence of catalyst content, four levels of Phencat 15 (4, 6, 8 and 10% by weight of total resin), were used in each formulation. At optimum catalyst content (8% for both resins A and B) mixes with five levels of filler to resin ratios were prepared in order to investigate the effect of resin and/or filler content (Table I). The ratios employed were 4:1, 5:1, 6:1, 7:1 and 8:1 by weight of total filler to resin content. With the two highest ratios proportionate weights of resin to furfuryl alcohol mixture was used to reduce the viscosity of the resin thus allowing a higher ratio of filler to resin to be used.

It was expected that the presence of the correct amount of microfiller particles would fill any interstitial voids between the larger sand particles. The amount of microfiller present was proportionally decreased or increased, below or above its optimum design level present in the most desirable grading line (19.5% silica flour by weight of total filler). In these investigations the microfiller (silica flour) content was also varied between 15, 19.5 and 25% by weight of total filler (Table I). In addition to silica flour, china clay and spheriglass 5000 were also used as microfillers. The required amount of these microfillers was calculated in terms of the volume equivalent to 19.5% silica flour in the mix design.

2.2. Specimen preparation and testing

The weight of silica sand fillers, microfillers, phenolic resin, relevant catalyst and furfuryl alcohol required

TABLE I Mix formulations of specimens used in double torsion tests

Mix	Filler formulation (%)					Resin type	Catalyst type & ratio (%)	Resin: filler ratio	Resin: furfuryl ratio
	Sands				Microfiller				
	2.4 mm	1.2 mm	600 μm	300 μm	150 μm				
E1	36.8	16.0	15.7	12.0	Silica flour, ~19.5	J50/010L (BP)	Phencat 15, ~8	4:1 5:1 6:1 7:1 8:1	– – – 80:20 60:40
E1	36.8	16.0	15.7	12.0	Silica flour, ~19.5	J50/010L (BP)	Phencat 15, ~4 ~6 ~10	6:1	– – –
E3	38.9	16.9	16.6	12.7	Silica flour, ~15.0	J50/010L (BP)	Phencat 15, ~8	6:1	–
E4	34.3	14.9	14.6	11.2	Silica flour, ~25	J50/010L (BP)	Phencat 15, ~8	6:1	–
E_{cc}	36.8	16.0	15.7	12.0	China clay, ~19.5	J50/010L (BP)	Phencat 15, ~8	6:1	–
E_{sg}	36.8	16.0	15.7	12.0	Spheriglass, ~19.5	J50/010L (BP)	Phencat 15, ~8	6:1	–
E1	36.8	16.0	15.7	12.0	Silica flour, ~19.5	IR1271 (Fordath)	CS-30, ~8	4:1 5:1 6:1 7:1 8:1	– – – 80:20 60:40
G2	–	64.0	–	11.0	Silica flour, ~25	J50/010L (BP)	Phencat 15, ~8	4:1 5:1 6:1 7:1	– – – 80:20

for each mix was measured to within 0.1 g. All formulations were based upon the requirement that specimens should achieve the same bulk density of 2.15 $Mg\,m^{-3}$. Each mix was therefore designed for the volume required to achieve the desired specimen thickness. For each test variable, sufficient constituents were weighed to produce three specimens $600 \times 100 \times 8\ mm^3$. The measured fillers (dry weights) were initially introduced into a Hobart mixer for a period of 5 min. The required weight of catalyst was then added and mixing continued for a further 3 min. During this stage the temperature was monitored using a thermocouple in order to maintain a constant temperature. This avoided accelerating the reaction when the resin was introduced, thereby maintaining a constant reaction time with respect to corresponding catalyst levels.

Each mix was cast into three rectangular steel moulds of $600 \times 100 \times 20\ mm^3$ internal dimensions made from 10 mm thick steel plate. A polytetrafluoroethane (PTFE) coated glass cloth was bonded to the top and bottom faces. The other surfaces were treated with a proprietary mould release spray.

The prepared resin and/or resin/furfuryl alcohol mixture was added to the catalysed filler and mixed at room temperature for a further 90 s until homogeneous. The mixture was then poured quickly into the prepared moulds and compacted with the aid of a vibrating table and levelled off to premarked depths. The lid of the mould was then fitted with any necessary spacers in position. Weights were placed on top of the lid, sufficient to produce a pressure of approximately 6500 Pa, which assisted setting. It also allowed any excess mixture to be extruded through bleed holes in the mould.

A period of 24 h was allowed for setting of the specimens subject to pressure at room temperature, except for mixes containing 4% catalyst which required the application of both heat and pressure. These were placed in an air oven at 80 °C for an initial period of 2 h. All moulds were stripped off after 24 h and the set specimens placed in an oven at 120 °C for 2 h post-curing. After the samples had been removed from the oven and cooled to room temperature, each was marked and cut into three almost equal rectangular plates nominally $198 \times 100 \times 8\ mm^3$ using a diamond tipped cutting wheel.

Double torsion specimens were produced in the form of rectangular plates approximately $200 \times 100 \times 8\ mm^3$ with shallow cast in grooves. These were made by incorporating polyvinylchloride (PVC) strips $600 \times 2 \times 1\ mm^3$ along the mid top and bottom faces of the moulds, in order to ensure that the crack propagated along the central axis of the plate. A single groove has been used with this test on other materials [14, 15, 18–22], but in this work two grooves were found to be necessary in order to facilitate satisfactory precracking.

At one end of the double torsion specimens, a notch 15 mm in length was introduced using a diamond tipped cutting wheel, shown schematically in Fig. 1. Precracking was achieved by using a wedge-indentation technique which has previously been shown to produce stable precracks with crack tips that are

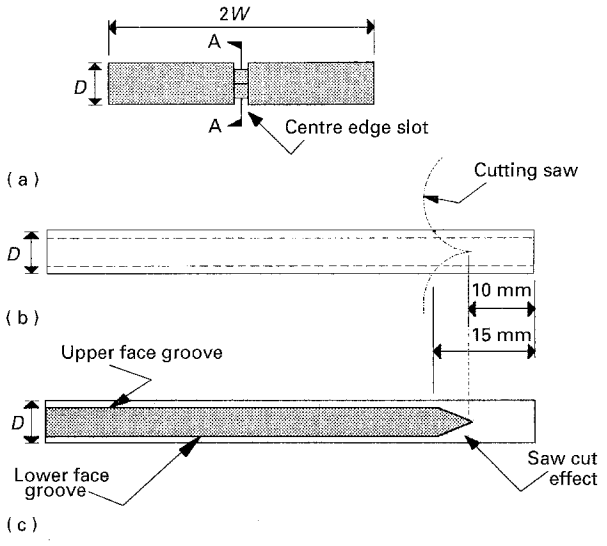

Figure 1 Details of centre grooves and centre edge slot. (a) end view, (b) side view and (c) Section A–A (parameters defined in Equation 1).

sharp and stress free [23]. A hardened steel 30° wedge was introduced into the notch at a constant crosshead displacement of 0.5 $mm\,min^{-1}$ using an Instron 1195 testing machine. The machine was stopped as soon as a load drop was detected on the load-displacement trace which indicated the initiation of a precrack. At the same time this process was monitored visually using a magnifying glass. In order to facilitate this, the centre grooves close to the notch were painted white prior to precracking.

The double torsion test specimen and its loading geometry are illustrated schematically in Fig. 2. The specimen was supported on two 200 mm long parallel 10 mm diameter steel rollers, 90 mm apart, resting on longitudinal grooves in a 20 mm thick supporting plate. This rested on the compression load cell of the Instron 1195 testing machine. Loading was applied via two parallel 10 mm thick plates with 5 mm radii at the point of contact with the specimen, positioned 19 mm apart. These were attached to an upper plate, at the centre top face of which a steel sphere was located in a semispherical nest. Immediately above this bearing was the second steel plate which was attached to the bottom face of the Instron crosshead. The arrangement is illustrated schematically in Fig. 3. Loading was applied at a crosshead speed of 2 $mm\,min^{-1}$. The load versus displacement of the crosshead was recorded directly on an x–y plotter which could be read to the nearest 2.5 N and 0.005 mm, respectively.

2.3. Flexural testing

Flexural properties were investigated using specimens in the form of rectangular coupons tested under four point loading as shown by Fig. 4. Steel and polypropylene moulds having internal dimensions of 600×100 mm with 4–10 mm adjustable depths were constructed for casting purposes. Specimens were produced in a similar manner to those used for the double torsion tests.

Prior to testing, each specimen had its geometrical dimensions carefully measured before being placed in

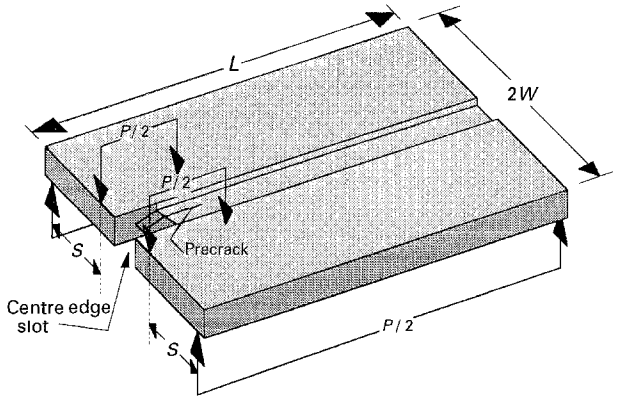

Figure 2 The double torsion test specimen and the loading geometry (parameters defined in Equation 1).

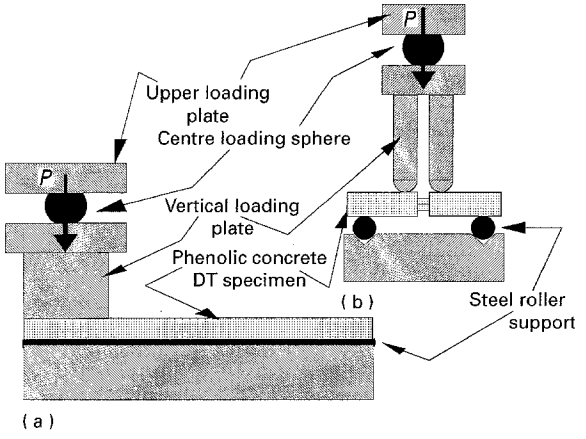

Figure 3 Schematic arrangement of the double torsion apparatus. (a) elevation, and (b) end view.

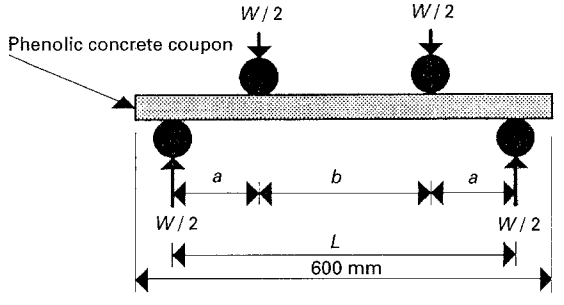

Figure 4 Phenolic concrete coupon specimen and the loading geometry (four point loading on Instron 1195 testing machine). The parameter a is the distance between the inner and the outer load rollers. The parameter $b = 2a$.

a test rig mounted on an Instron type 1195 testing machine. The test rig was attached directly to a load cell which rested on top of the Instron spreader beam and the base of the rig was connected to the Instron crosshead through universal hinge joints. The specimens were tested subject to four point loading under constant spans between the loading positions (see Fig. 4). Each test was conducted at a constant crosshead displacement of 20 mm min^{-1}. The load–deflection response of each specimen was monitored on an x–y recorder. From the load–deflection plots, the slope and the ultimate sustained load at failure were obtained. These were used to determine flexural modulus and ultimate flexural strength in terms of its extreme fibre tension stress for each specimen using simple bending theory [16].

Samples were taken from some specimens following testing and their densities measured using the Archimedes' method. The surface topography of the fracture surfaces of some of the tested flexural specimens was also studied using a Cambridge S600 scanning electron microscope (SEM).

3. Results

The load–displacement curves of all the double-torsion specimens exhibited a brittle crack propagation behaviour. For specimens made of low filler : resin ratio, the curves became almost flat at maximum load, the displacement increasing in a stable manner at constant load. As the filler : resin ratio increased, the corresponding curves changed from stable to stick–slip.

Failure of the specimens occurred with a sudden drop in load followed by complete separation of the sample into two pieces. The crack in low filler : resin ratio samples propagated centrally along the specimen axis with no evidence of crack arrest having taken place. This is usually described as "stable" crack

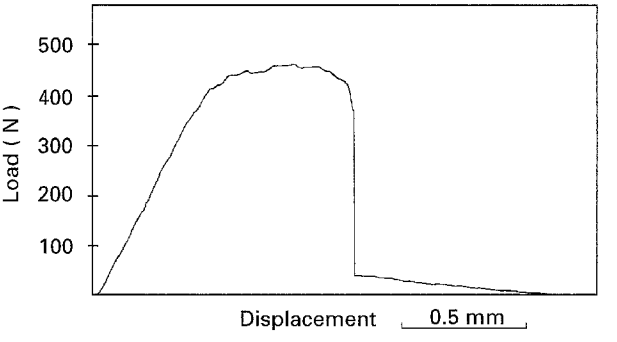

Figure 5 Typical recorded plot of load versus displacement from double torsion test for a mix ratio of 4 : 1.

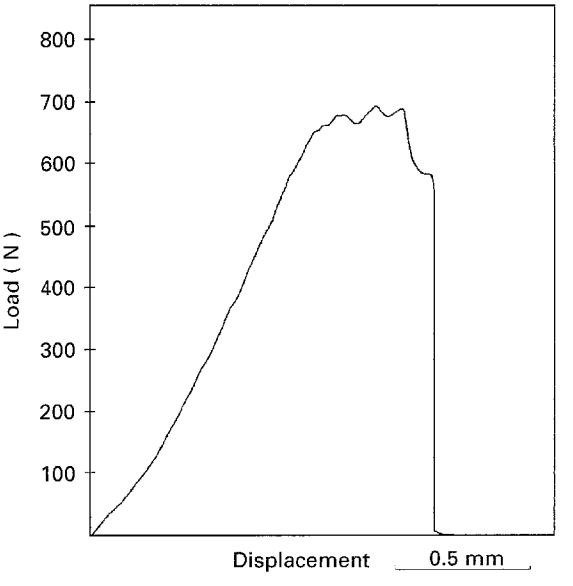

Figure 6 Typical recorded plot of load versus displacement from double torsion test for a mix ratio of 8 : 1.

growth and is illustrated in Fig. 5 for a mix ratio of 4:1. As the filler:resin ratio increased beyond 6:1 the crack propagation mode changed from "stable" to "unstable" crack growth exhibiting defined propagation and arrest stages. A typical load–displacement trace showing this effect is presented in Fig. 6 for a mix ratio of 8:1. G_{Ic} was calculated from the maximum load, P_{max}, using the following equation [24]

$$G_{Ic} = \frac{P_{max}^2}{2D}\frac{(1+\upsilon)}{E}\frac{S^2}{ZWD^3} \quad (1)$$

where P_{max} is the load at the onset of crack propagation, D is the full specimen thickness, $2W$ is the total specimen width, S is the distance between the loading point and the support roller, Z is a function of W/D ratio [25], E is Young's modulus and υ is Poisson's ratio.

The data of Table II, which relate to resin A, show that the fracture energy increases with filler:resin ratio. These values are in good agreement with those of the specimens prepared using resin B presented in Table III. The variation in G_{Ic} and (estimated) fracture toughness K_{Ic}, values are presented graphically in Fig. 7a, b, respectively, as a function of filler:resin ratio. It can be seen that the pattern of increase in G_{Ic} values with increase in filler content of both resin composites is similar, whereas this is not generally so for their corresponding calculated K_{Ic} values.

Table IV shows that there is an increase in toughness values as the catalyst content of the formulation increases. Table V shows how these values vary as a function of microfiller content for similar mix formulation and, from Table VI, there is little evidence to suggest that silica flour has a superior effect on the fracture toughness of the phenolic concretes compared to other microfillers.

From Table V it can be seen that the microfiller content (silica flour) in the mix composition seems to have a significant effect on the fracture toughness of the phenolic concrete. It was also found from the flexural tests to affect strength and stiffness values. At 19.5% loading the filler mix grading curve follows the Fuller grading curve and hence provides a more uniformly packed, i.e. more homogeneous, filler within the matrix. Above or below this level (Table V) toughness is seen to decrease.

4. Discussion

One possible reason for the observed increase in the G_{Ic} values with mix ratio is that the crack will propagate through or around more filler grains as the filler content increases. Thus, more energy could be

TABLE II Filler:Resin ratio effect for resin A (J50/010L)

Mix ratio	Sample	Dimensions (mm)		$Z=f(W/D)$		Failure load, $P_{max}(N)$	Fracture energy, G_{Ic} (J m^{-2})		Stress intensity factor, K_{Ic} (MN m$^{-3/2}$)		Defect size, a (mm)
		Length	Depth	W/D	Z						
4:1	a	200.75	8.11	6.17	0.296	470.0	186.9	[a]Av.	1.7		
	b	197.00	8.02	6.23	0.296	442.5	173.2	180.7	1.7	Av.	1.88
	c	204.50	7.63	6.55	0.298	400.0	171.6		1.7	1.70	
	d	194.75	7.80	6.41	0.297	427.5	180.1	[b]S.d.	1.7		
	e	200.25	7.90	6.33	0.297	447.5	187.5	± 7.0	1.7		
	f	195.00	8.13	6.15	0.296	470.0	185.0		1.7		
5:1	a	202.00	8.03	6.23	0.296	490.0	192.1	Av.	1.8		
	b	197.00	8.49	5.89	0.295	520.0	173.7	187.2	1.7	Av.	1.70
	c	196.00	8.01	6.24	0.296	470.0	196.4		1.9	1.82	
	d	198.00	8.18	6.11	0.296	500.0	184.7	S.d.	1.8		
	e	198.00	8.44	5.92	0.296	520.0	177.8	± 10.2	1.8		
	f	201.00	8.08	6.19	0.295	505.0	198.6		1.9		
6:1	a	194.00	7.99	6.26	0.296	508.0	199.9	Av.	1.9		
	b	200.50	7.92	6.31	0.297	495.0	196.1	197.0	1.9	Av.	1.82
	c	201.50	7.63	6.55	0.298	460.0	195.9		1.9	1.90	
	d	199.75	8.03	6.23	0.296	510.0	197.6	S.d.	1.9		
	e	199.50	8.00	6.25	0.296	500.0	192.8	± 2.6	1.9		
	f	200.75	8.05	6.21	0.296	515.0	199.5		1.9		
7:1	a	198.50	8.63	5.79	0.294	625.0	204.8	Av.	2.0		
	b	201.50	8.51	5.88	0.295	630.0	219.4	211.9	2.1	Av.	1.61
	c	196.75	8.13	6.15	0.296	563.5	210.0		2.1	2.08	
	d	200.75	8.42	5.94	0.295	610.0	214.6	S.d.	2.1		
	e	200.50	8.59	5.82	0.294	630.0	212.0	± 4.9	2.1		
	f	195.00	8.57	5.83	0.294	625.0	210.6		2.1		
8:1	a	202.00	8.51	5.88	0.295	620.0	202.5	Av.	2.1		
	b	198.00	8.60	5.81	0.294	677.0	232.0	213.6	2.2	Av.	1.54
	c	195.50	8.50	5.88	0.295	632.0	211.4		2.1	2.12	
	d	198.00	8.40	5.95	0.295	620.0	213.3	S.d.	2.1		
	e	198.00	8.55	5.85	0.295	640.0	211.7	± 9.9	2.1		
	f	197.50	8.57	5.83	0.294	640.0	210.5		2.1		

[a] Av., average.
[b] S.d., standard deviation.

TABLE III Filler: Resin ratio effect for resin B (IR1271)

Mix ratio	Sample	Dimensions (mm)		$Z = f(W/D)$		Failure load, $P_{max}(N)$	Fracture energy, G_{Ic} (J m^{-2})		Stress intensity factor, K_{Ic} (MN m$^{-3/2}$)		Defect size, a (mm)
		Length	Depth	W/D	Z						
4:1	a	198.75	7.96	6.28	0.296	495.0	196.7	[a]Av.	1.9		2.14
	b	199.00	8.12	6.16	0.296	505.0	189.1	187.8	1.8	Av.	
	c	199.50	8.04	6.22	0.296	495.0	189.0		1.8	1.82	
	d	198.75	8.10	6.17	0.296	497.5	185.3	[b]S.d.	1.8		
	e	199.25	8.02	6.23	0.296	490.0	187.1	± 5.6	1.8		
	f	198.00	7.98	6.27	0.296	480.0	179.5		1.8		
5:1	a	199.75	8.24	6.07	0.295	520.0	189.7	Av.	1.9		2.03
	b	198.00	8.15	6.13	0.296	510.0	190.0	191.7	1.9	Av.	
	c	200.25	8.16	6.13	0.296	500.0	181.7		1.8	1.87	
	d	199.50	7.96	6.28	0.296	485.0	188.9	S.d.	1.8		
	e	200.00	7.88	6.35	0.297	500.0	208.3	± 8.8	1.9		
	f	199.00	7.97	6.27	0.296	490.0	191.8		1.9		
6:1	a	198.75	8.03	6.23	0.296	505.0	197.7	Av.	1.9		
	b	199.50	8.11	6.17	0.296	505.0	190.0	201.7	1.9	Av.	1.80
	c	198.50	8.21	6.09	0.296	550.0	214.6		2.0	1.92	
	d	198.75	8.25	6.06	0.295	540.0	203.6	S.d.	1.9		
	e	198.50	8.09	6.18	0.296	520.0	203.5	± 8.1	1.9		
	f	197.75	8.12	6.16	0.296	520.0	200.5		1.9		
7:1	a	197.50	8.41	5.95	0.295	565.0	206.4	Av.	1.9		
	b	199.50	8.78	5.69	0.294	615.0	206.6	208.0	1.9	Av.	1.45
	c	198.75	8.22	6.08	0.296	540.0	205.9		1.9	1.93	
	d	197.75	8.14	6.14	0.296	535.0	210.1	S.d.	1.9		
	e	198.50	8.36	5.98	0.295	565.0	211.4	± 2.8	2.0		
	f	199.00	8.46	5.91	0.295	580.0	212.4		2.0		
8:1	a	200.75	8.12	6.16	0.296	540.0	216.2	Av.	2.0		
	b	196.75	8.63	5.79	0.294	595.0	207.1	220.7	1.9	Av.	1.27
	c	199.50	8.42	5.94	0.295	590.0	224.0		2.0	1.98	
	d	201.00	8.38	5.97	0.295	585.0	224.4	S.d.	2.0		
	e	200.50	8.49	5.89	0.295	600.0	224.1	± 7.8	2.0		
	f	201.50	8.21	6.09	0.296	567.0	228.4		2.0		

[a] Av., average.
[b] S.d., standard deviation.

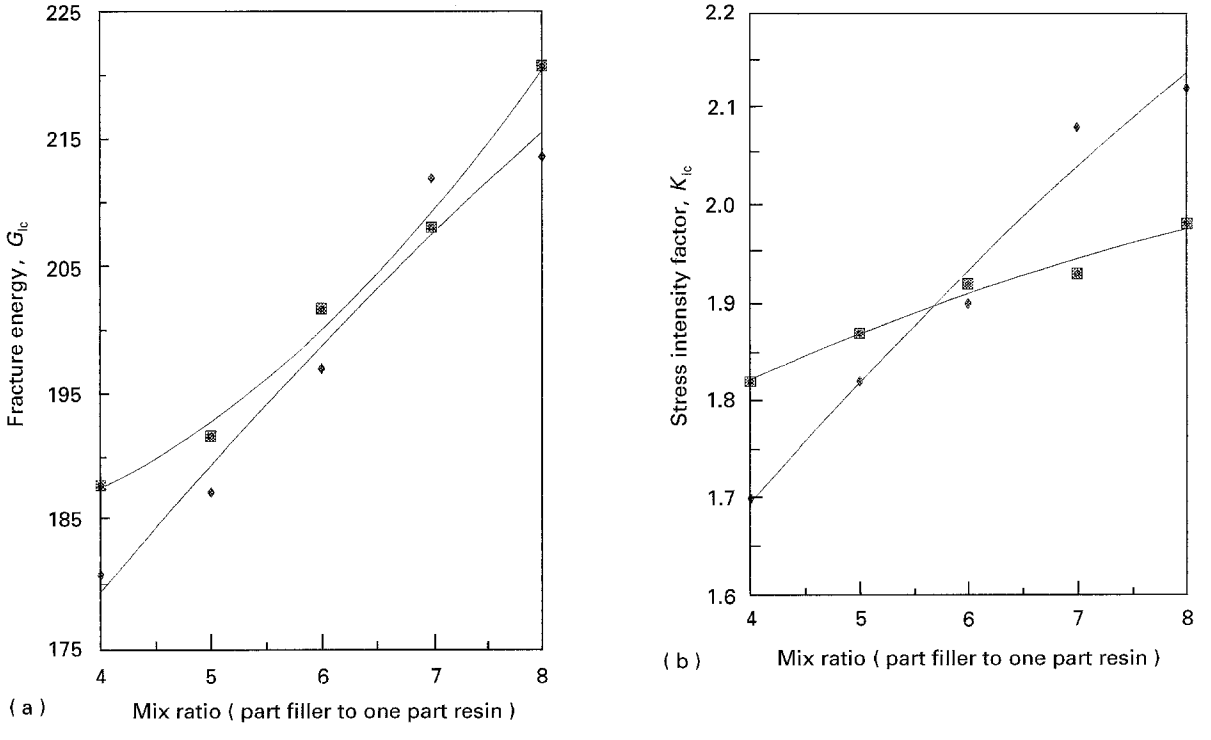

Figure 7(a) Fracture energy, G_{Ic}, and (b) stress intersit factor, K_{Ic}, as a function of mix ratio: (◆) BP, J$_5$0/010L, (■) Fordath IR 1271.

TABLE IV Catalyst content effect

Catalyst content (%)	Sample	Dimensions (mm)		$Z=f(W/D)$		Failure load, $P_{max}(N)$	Fracture energy, G_{Ic} (J m^{-2})		Stress intensity factor, K_{Ic} (MN m$^{-3/2}$)		Defect size, a (mm)
		Length	Depth	W/D	Z						
4	a	198.00	8.47	5.90	0.295	500.0	168.6	[a]Av.	1.7		1.43
	b	192.00	8.19	6.11	0.296	452.0	157.0	156.6	1.6	Av.	
	c	199.00	8.47	5.90	0.295	465.0	145.8	[b]S.d.	1.5	1.60	
	d	198.00	8.20	6.10	0.296	450.0	154.9	± 9.4	1.6		
6	a	195.75	8.70	5.75	0.294	540.0	168.6	Av.	1.7		2.00
	b	196.75	8.75	5.71	0.294	530.0	158.8	162.8	1.7	Av.	
	c	195.00	8.69	5.75	0.294	522.0	158.3		1.7	1.68	
	d	195.00	9.09	5.50	0.293	560.0	152.7	S.d.	1.6		
	e	196.25	8.85	5.65	0.294	550.0	163.3	± 8.1	1.7		
	f	198.75	8.49	5.89	0.295	525.0	175.2		1.7		
8	a	194.00	7.99	6.26	0.296	508.0	199.9	Av.	1.9		
	b	200.50	7.92	6.31	0.297	490.0	196.1	197.0	1.9	Av.	1.82
	c	201.50	7.63	6.55	0.298	465.0	195.9		1.9	1.9	
	d	199.75	8.03	6.23	0.296	510.0	197.6	S.d.	1.9		
	e	199.50	8.00	6.25	0.296	500.0	192.8	± 2.6	1.9		
	f	200.75	8.05	6.21	0.296	515.0	199.5		1.9		
10	a	200.25	8.57	5.83	0.294	620.0	207.5	Av.	2.0		
	b	198.75	8.89	5.62	0.294	665.0	206.2	203.2	2.0	Av.	1.66
	c	201.75	8.45	5.92	0.295	600.0	204.9		2.0	2.0	
	d	195.75	8.87	5.64	0.294	650.0	198.8	S.d.	2.0		
	e	199.50	9.06	5.52	0.293	690.0	195.2	± 7.8	2.0		
	f	198.75	9.02	5.54	0.293	665.0	206.5		2.0		

[a] Av., average.
[b] S.d., standard deviation.

TABLE V Microfiller content effect

Microfiller content %	Sample	Dimensions (mm)		$Z=f(W/D)$		Failure load, $P_{max}(N)$	Fracture energy, G_{Ic} (J m^{-2})		Stress intensity factor, K_{Ic} (MN m$^{-3/2}$)		Defect size, a (mm)
		Length	Depth	W/D	Z						
Silica flour ~15	a	197.00	9.18	5.45	0.293	530.0	126.2	[a]Av.	1.4		
	b	196.00	8.71	5.74	0.294	495.0	135.4	137.7	1.5	Av.	1.48
	c	198.00	8.79	5.69	0.294	525.0	146.9		1.5	1.48	
	d	196.00	8.53	5.86	0.295	480.0	138.0	[b]S.d.	1.5		
	e	194.50	8.95	5.59	0.293	530.0	139.7	± 6.8	1.5		
	f	196.00	8.85	5.65	0.294	520.0	140.2		1.5		
Silica flour ~19.5	a	194.00	7.99	6.26	0.296	508.0	199.9	Av.	1.9		
	b	200.50	7.92	6.31	0.297	495.0	196.1	197.0	1.9	Av.	1.82
	c	201.50	7.63	6.55	0.298	460.0	195.9		1.9	1.9	
	d	199.75	8.03	6.23	0.296	510.0	197.6	S.d.	1.9		
	e	199.50	8.00	6.25	0.296	500.0	192.8	± 2.6	1.9		
	f	200.75	8.05	6.21	0.296	515.0	199.5		1.9		
Silica flour ~25	a	202.50	9.20	5.43	0.293	540.0	129.9	Av.	1.5		1.34
	b	192.00	9.55	5.24	0.292	555.0	118.6	128.8	1.4	Av.	
	c	191.00	9.08	5.51	0.293	530.0	131.9		1.5	1.47	
	d	200.00	8.76	5.71	0.294	505.0	137.8	S.d.	1.5		
	e	200.75	9.30	5.38	0.293	550.0	129.1	± 6.5	1.5		
	f	199.55	9.24	5.41	0.293	535.0	125.3		1.4		

[a] Av., average.
[b] S.d., standard deviation.

consumed as a result of the potentially larger true fracture area. Examination of the SEM images of the fracture surfaces shows that crack propagation appears to take place through sand grains (Fig. 8) which suggests that the filler is well bonded to the matrix resin.

Table IV indicates that there is an increase in toughness values as the catalyst content of the formulation increases. This may be due to the fact that the resin matrix in the exothermic polymerization reaction produces a greater rate and quantity of condensation with increasing catalyst level. Earlier work has suggested that more spherical voids are produced [16] as well as the possibility of stronger and larger cross links. The presence of spherical microvoids (Figs. 8 and 9) will undoubtedly influence crack propagation behaviour.

TABLE VI Microfiller type effect

Microfiller type	Sample	Dimensions (mm)		$Z = f(W/D)$		Failure load, $P_{max}(N)$	Fracture energy, G_{Ic} (J m^{-2})		Stress intensity factor, K_{Ic} (MN m$^{-3/2}$)		Defect size, a (mm)
		Length	Depth	W/D	Z						
China clay (D)	a	193.50	8.06	6.20	0.296	520.0	202.4	[a]Av.	1.9		2.05
	b	205.50	7.94	6.30	0.296	500.0	198.7	200.8	1.9	Av.	
	c	191.00	8.38	5.97	0.295	540.0	187.4		1.9	1.92	
	d	194.75	8.42	5.94	0.295	565.0	201.3	[b]S.d.	1.9		
	e	200.25	8.22	6.08	0.296	540.0	201.8	$\pm$ 8.3	1.9		
	f	195.00	8.07	6.20	0.296	535.0	213.2		2.0		
Spheriglass 5000	a	200.00	7.65	6.54	0.293	470.0	205.9	Av.	1.9		
	b	198.75	7.69	6.50	0.297	485.0	211.8	210.3	2.0	Av.	1.98
	c	192.25	7.33	6.82	0.299	450.0	219.4		2.0	1.97	
	d	198.00	7.56	6.61	0.298	455.0	198.9	S.d.	1.9		
	e	198.00	7.64	6.54	0.297	485.0	217.4	$\pm$ 7.6	2.0		
	f	201.00	7.68	6.51	0.297	480.0	208.5		2.0		
Silica flour	a	194.00	7.99	6.26	0.296	508.0	199.9	Av.	1.9		
	b	200.50	7.92	6.31	0.297	495.0	196.1	197.0	1.9	Av.	1.82
	c	201.50	7.63	6.55	0.298	460.0	195.9		1.9	1.90	
~19.5%	d	199.75	8.03	6.23	0.296	510.0	197.6	S.d.	1.9		
	e	199.50	8.00	6.25	0.296	500.0	192.8	$\pm$ 2.6	1.9		
	f	200.75	8.05	6.21	0.296	515.0	199.5		1.9		

[a] Av. average.
[b] S.d., standard deviation.

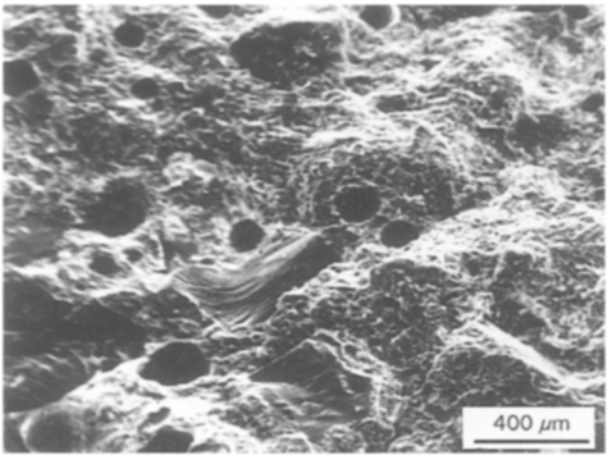

Figure 8 Scanning electron fractograph showing that good adhesion between the sand grains and the resin matrix has been achieved.

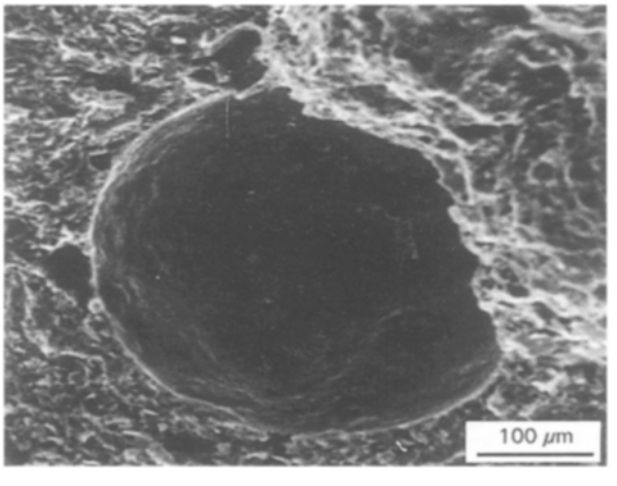

Figure 9 Scanning electron fractograph showing the presence of spherical microvoids.

Although the use of silica flour in the mix matrix has been previously shown to have a beneficial effect on flexural strength of the phenolic concrete in comparison to the use of other microfillers [16], there is little evidence from this work to suggest that this is as a result of changes to fracture toughness. However, the K_{Ic} value of the material depends on the microstructural feature and is generally insensitive to the chemical properties of the surrounding environment.

The fracture toughness of the gap-graded specimens (Table VII) is lower than those using the Fuller grading mix design (Tables III and VIII). Therefore, the mix: filler grading to satisfy the Fuller grading specification seems to be the best design in optimizing the fracture toughness of the composite. This may result from a less homogeneous filler packing than in the Fuller specification. It has been shown that for concrete, larger grain sizes result in higher values of fracture energy. Fracture toughness is influenced by increases in the lower range of the grain size distribution, with no significant effect being shown by changes in the larger grain sizes [26]. However, with graphite for example, it has been shown [27] that the mode of failure precludes its description as a perfectly brittle material. In this case crack growth is independent of particle size and total fracture strain increases with reduced particle size. In the gap-grading mixes reported in this work the larger sand grains, i.e. those passing a 2.4 mm BS sieve, are not present, as they are included in Fuller grading mixes. It may therefore be valid to assume that the lower toughness values in these specimens are due to the exclusion of the larger grain size. By a mix ratio of 7:1 of the gap-grading mix (Table VII) the fracture toughness value has decreased. It seems reasonable to suppose that this is due to a lack of resin to fill the interstitial voids between the larger particles, which results in the

TABLE VII Filler:Resin ratio effect (gap-grading mix) for resin J50/010L

Mix ratio	Sample	Dimensions (mm)		$Z = f(W/D)$		Failure load, P_{max}(N)	Fracture energy, G_{Ic}(J m^{-2})		Stress intensity factor, K_{Ic} (MN m$^{-3/2}$)		Defect size, a (mm)
		Length	Depth	W/D	Z						
4:1	a	196.25	8.52	5.88	0.295	480.0	157.0	[a]Av.	1.6		
	b	195.75	8.50	5.87	0.295	485.0	158.8	153.6	1.6	Av.	1.79
	c	196.00	9.14	5.47	0.293	540.0	149.7		1.6	1.60	
	d	195.75	9.13	5.48	0.293	537.5	148.9	[b]S.d.	1.6		
	e	195.25	9.00	5.56	0.293	530.5	153.6	± 4.4	1.6		
5:1	a	195.00	8.55	5.85	0.295	502.5	168.1	Av.	1.7		
	b	195.50	8.91	5.61	0.294	525.0	156.1	160.2	1.6	Av.	1.63
	c	196.75	8.54	5.85	0.295	495.0	163.9		1.6	1.62	
	d	196.25	9.05	5.52	0.293	540.0	155.7	S.d.	1.6		
	e	195.25	9.01	5.55	0.293	538.0	157.3	± 5.5	1.6		
6:1	a	195.75	8.71	5.74	0.294	510.5	161.6	Av.	1.6		
	b	195.25	8.86	5.64	0.294	520.0	156.6	163.2	1.6	Av.	1.37
	c	195.25	8.46	5.91	0.295	510.0	179.3		1.7	1.62	
	d	198.00	9.02	5.54	0.293	540.0	157.8	S.d.	1.6		
	e	195.50	8.85	5.65	0.294	525.0	160.7	± 9.2	1.6		
7:1	a	196.50	8.40	5.95	0.295	465.0	154.5	Av.	1.6		
	b	195.00	8.92	5.61	0.294	515.0	149.6	152.4	1.6	Av.	1.16
	c	195.75	8.73	5.73	0.294	505.0	147.7		1.6	1.60	
	d	195.75	8.86	5.64	0.294	515.0	153.6	S.d.	1.6		
	e	196.50	8.95	5.59	0.293	530.0	156.8	± 3.7	1.6		

[a] Av., average.
[b] S.d., standard deviation.

TABLE VIII Properties of specimens used in double torsion tests

Mix	Mix composition				Workability	Density (Mg m^{-3})	Flexural tests		Tensile tests	
	Resin type	Catalyst and ratio (%)	Resin: filler ratio	Resin: furfuryl ratio			Strength (MPa)	Modulus (GPa)	Strength (MPa)	Modulus (GPa)
E1	J50/010L (BP)	Phencat 15, ~8	4:1	–	Very	2.09	22.1	23.9	5.9	14.8
			5:1	–	Very	2.12	24.9	25.1	6.1	16.3
			6:1	–	Workable	2.14	25.1	25.9	7.0	17.1
			7:1	80:20	Workable	2.19	29.3	27.5	7.7	18.7
			8:1	60:40	Workable	2.22	30.5	28.9	7.9	19.6
E1	J50/010L (BP)	Phencat 15,	6:1							
		~4		–	Workable	2.15	23.9	24.5	5.6	15.6
		~6		–	Workable	2.13	21.3	23.5	6.1	16.4
		~10		–	Workable	2.14	27.7	28.8	7.7	18.7
E3	J50/010L (BP)	Phencat 15, ~8	6:1	–	Very	2.10	21.7	22.2	4.7	14.5
E4	J50/010L (BP)	Phencat 15, ~8	6:1	–	Workable	2.17	22.7	24.0	5.4	15.3
E_{cc}	J50/010L (BP)	Phencat 15, ~8	6:1	–	Workable	2.12	24.3	24.0	7.0	17.1
E_{sg}	J50/010L (BP)	Phencat 15, ~8	6:1	–	Workable	2.15	25.2	26.0	7.2	17.1
E1	IR1271 (Fordath)	CS-30, ~8	4:1	–	Very	2.05	22.2	23.4	–	–
			5:1	–	Very	2.11	23.4	24.6	6.6	16.7
			6:1	–	Very	2.14	25.6	27.9	7.1	16.9
			7:1	80:20	Workable	2.16	28.6	29.4	–	–
			8:1	60:40	Workable	2.20	31.4	32.4	–	–
G2	J50/010L (BP)	Phencat 15, ~8	4:1		Very	2.08	21.3	24.6	–	–
					Very	2.10	22.6	24.6	–	–
					Very	2.13	24.7	25.7	5.9	14.9
					Very	2.15	26.5	27.9	5.9	15.6

development of star shaped voids with resulting stress concentration effects.

From the average fracture toughness values the sizes of possible defects in the phenolic concrete matrix were calculated using the following expression [28]

$$K_{Ic} = \psi\sigma(\pi a)^{1/2}$$

where σ is the nominal (flexural) strength of coupon specimens, a is the inherent defect size, and ψ is a dimensionless shape factor.

The calculated defect size in all the specimens made from Fuller grading mixes (Tables III–VIII), falls below the maximum grain size, i.e. maximum size passing BS sieve 2.4 mm. This indicates that the mix and casting processes have been successfully controlled and no defects larger than those associated with the biggest filler grains (sands) are present in the composite. However, the calculated defect sizes in the specimens constructed from the gap-grading mixes seems to be somewhat larger than the maximum sand grains present in the matrix, i.e. maximum size passing BS sieve 1.2 mm. Therefore, using a gap-grading mix may prevent the production of a homogeneous phenolic concrete which may cause a reduction in fracture toughness of the material.

5. Conclusions

The use of double-torsion specimens having centre face shallow grooves has been successfully used in determining the fracture energy, G_{Ic}, of phenolic concrete from which fracture toughness, K_{Ic}, values were calculated. Fracture toughness was found to be in the range 1.47–2.12 MN m$^{-3/2}$, with the fracture energy as high as 220 J m^{-2}. It was found that phenolic concrete is tougher and stiffer than ordinary Portland cement based concrete and is equally as tough as polyester concrete. The fracture energy, G_{Ic}, appears to be affected by filler: resin ratio, generally increasing with this ratio. Precracking using the wedge-indentation technique can be successfully employed with double torsion specimens with a centre edge saw cut as a starter crack. This technique provided sharp precracking with stable "brittle" crack propagation.

It has been shown that the Fuller grading design provides an optimum mix which results in the highest fracture toughness values. A comparison between this type of mix to a gap-grading mix suggested that defects are evident in the latter which affect the mechanical properties. Resin type has no significant effect on fracture toughness regardless of the type of compatible microfiller used. The level of the acid catalyst which can be successfully used in phenolic concrete has been shown to be determined by the mix and casting process, type of catalyst and temperature.

References

1. "Synthetic Resins for Building Construction", International Symposium on Experimental Research on New Developments brought by Synthetic Resins to Building Techniques, Vols 1 and 2 (1967).
2. "Polymers in Concrete", ACI Committee 548 (American Concrete Institute, Detroit, MI, 1977). pp 1–419.
3. "Polymers in Concrete", International Symposium, Publication SP-58, (American Concrete Society, Detroit, MI, 1978).
4. "Polymers in Concrete", First International Symposium on Polymer Concrete, London, 1975 (Construction Press Ltd, London, 1976).
5. "Polymers in Concrete", Proceedings of the Second International Congress on Polymers in Concrete, Austin TX November 1978 edited by B. W. Staynes (American Concrete Institute, 1978).
6. "Polymers in Concrete", Proceedings of the Third International Congress on Polymers in Concrete, May 1981 Koryama Japan edited by B. W. Staynes, Vols 1 and 2 (American Concrete Institute, 1981).
7. "Polymers in Concrete", Proceedings of the Fourth International Congress on Polymers in Concrete (Institut für Spanende Technologic und Werkzengmachinen, Darmstadt, September 1984). edited by B. W. Staynes
8. "Polymers in Concrete", Proceedings of the Fifth International Congress on Polymers in Concrete The Production, Performance and Potential of Polymers in Concrete, Brighton, UK September 1984 edited by B. W. Staynes.
9. "Polymers in Concrete", Proceedings of the Sixth International Congress on Polymers in Concrete, (International Academic Publishers, Pergamon–CNPIEC, Tongji University, Shanghai, China, September 1990).
10. R. C. PRUSINSKI, in American Concrete Society, Publication SP-58 (American Concrete Institute, 1978) pp. 75–102.
11. G. M. SABNIS, H. G. HARRIS, R. N. WHITE and S. M. MIRZA, "Structural Modeling and Experimental Techniques" (Prentice Hall, Eaglewood Cliffs NJ, 1982) pp. 63–103.
12. A. KNOP and W. SCHEIB, "Chemistry and Application of Phenolic Resins" (Springer-Verlag, Berlin 1985) pp. 313.
13. A. KNOP and L. A. PILATO, "Phenolic Resins: Chemistry, Application, Performance and Future Directions" (Springer-Verlag, Berlin 1979).
14. T. V. PARRY, S. J. IGBINEDION and A. S. WRONSKI, in "Special Ceramics", Vol. 8, edited by S. P. Howlett and D. Taylor (Butterworth, London, 1986) pp. 281–286.
15. S. J. IGBINEDION, T. V. PARRY and A. S. WRONSKI, *Int. J. Adhesion & Adhesives* **7** (1987) 205.
16. A. A. SHARIATMADARI, PhD thesis, University of Durham (1992).
17. G. M. PARTON, A. A. SHARIATMADARI and R. G. HANSOM *Int. J. Cement, Composites & Lightweight Concrete* **11** (1989) 167.
18. C. G. ANNIS and J. S. CARGILL in "Fracture Mechanics of Ceramics", Vol. 4, edited by R. C. Bradt, D. P. H. Hasselman and F. F. Lange (Plenum Press, New York, 1978) pp. 737–734.
19. A. G. EVANS, *J. Mater. Sci.* **7** (1972) 1137.
20. P. W. R. BEAUMONT and J. R. YOUNG, *ibid.* **10** (1975) 1334.
21. T. A. MICHALSKE, M. SINGH and V. D. FRECHETTE, in "Fracture Mechanics for Ceramics, Rocks and Concrete" (American Society for Testing Materials, Philadelphia, PA, 1981) pp. 3–12.
22. M. H. LEWIS and B. S. B. KARUNARATNE, *ibid.* pp. 13–32.
23. E. A. ALMOND and B. ROEBUCK *ibid.* pp. 85–95.
24. A. J. KINLOCK and S. J. SHAW, "Developments in Adhesives", Vol. 2, edited by A. J. Kinlock (Applied Science, 1981) pp. 83–124.
25. S. P. TIMOSHENKO and J. N. GOODIER, "Theory of Elasticity", 3rd Edn (McGraw-Hill, New York 1984) p. 312.
26. A. BOCHENEK and G. PROKOPSKI, *Int. J. Fract.* **41** (1989) 197.
27. E. P. KENNEDY and C. R. KENNEDY, in Proceedings, 13th National Symposium on Fracture Mechanics, American Society for Testing Materials. Philadelphia, PA, 1980, pp. 303–315.
28. J. F. KNOTT, "Fundamentals of Fracture Mechanics" (Butterworth, London, 1973). pp 114–149

Received 8 September 1994
and accepted 7 June 1995